LA-3789-MS

LOS ALAMOS SCIENTIFIC LABORATORY
of the
University of California
LOS ALAMOS • NEW MEXICO

A Numerical Study of Excursions in UHTREX Loaded with Standard Fuel Elements

UNITED STATES
ATOMIC ENERGY COMMISSION
CONTRACT W-7405-ENG. 36

DISCLAIMER

LEGAL NOTICE

Printed in the United States of America. Available from
Clearinghouse for Federal Scientific and Technical Information
National Bureau of Standards, U. S. Department of Commerce
Springfield, Virginia 22151
Price: Printed Copy $3.00; Microfiche $0.65

LA-3789-MS
UC-80, REACTOR
TECHNOLOGY
TID-4500

LOS ALAMOS SCIENTIFIC LABORATORY
of the
University of California
LOS ALAMOS • NEW MEXICO

Report written: September 1967
Report distributed: January 24, 1968

A Numerical Study of Excursions in UHTREX Loaded with Standard Fuel Elements

by

John C. Vigil

THIS PAGE

WAS INTENTIONALLY

LEFT BLANK

A NUMERICAL STUDY OF EXCURSIONS IN UHTREX LOADED WITH STANDARD FUEL ELEMENTS

by

John C. Vigil

ABSTRACT

Preliminary numerical calculations of the response of the Ultra High Temperature Reactor Experiment (UHTREX) (loaded with standard fuel elements) to a wide range of reactivity inputs are presented. These calculations were done in support of a proposed series of excursion experiments whose main purpose is to determine the adequacy of calculational methods presently being used and to identify areas where the methods may need improvement. For example, the experiments would provide a test of the calculated fuel temperature coefficient in UHTREX and would contribute to the testing of nonseparable space-time neutron kinetics codes now being developed. These codes are needed for analysis of transients in UHTREX loaded with specially designed U-Th fuel elements and in other assemblies for transient studies in support of the High Temperature Gas-Cooled Reactor (HTGR) Program.

INTRODUCTION AND SUMMARY

Preliminary numerical calculations of the response of UHTREX,[1] loaded with standard fuel elements, to a wide range of reactivity inputs are reported here. The reactor was assumed to be initially at room temperature (300°K) and one watt delayed critical. The reactor was also assumed to be under one atmosphere of helium with no coolant flow, so the heat losses from the core to surrounding reflector regions during the transients can be neglected. Included in the calculations are:

a. A study of the effect of gross spatial variations in the power (unrodded critical mode) and in the reactivity coefficients,

b. A study of the effect of variation with temperature of the graphite heat capacity and reactivity coefficients,

c. A comparison of step inputs with detailed reactivity inputs due to rod withdrawal at 18 in./min,

d. A study of the effect of replacement of helium by nitrogen or a vacuum, and

e. A study of the sensitivity of the results to arbitrary changes in prompt-neutron generation time and reactivity coefficients.

These calculations were done in support of a proposed series of transient experiments in UHTREX. The main purpose of these experiments is to determine the adequacy of calculational methods presently being used and to identify areas where the methods may need improvement. For example, the experiments would provide a test of the calculated fuel temperature coefficient in UHTREX and would contribute to the testing of nonseparable space-time neutron kinetics codes now being developed. These codes are needed for analysis of transients in UHTREX loaded with specially designed U-Th fuel elements and in other assemblies for transient studies in support of the High Temperature Gas-Cooled Reactor (HTGR) Program.

The calculations indicate that the response of available instrumentation and the design rod withdrawal speed of 18 in./min in UHTREX are adequate for slow transients (reactivity inputs <$1). These slow transients can be used to obtain an experimental value for the fuel temperature coefficient. For the smaller reactivity inputs, replacement of the helium by nitrogen or a vacuum is found to aid considerably

in thermally isolating the fuel elements from the bulk moderator. It is important, for safety reasons, that the existence of the prompt shutdown mechanism in UHTREX be experimentally verified before a significant fission product inventory is accumulated. Thus, the slow transient experiments should be done with the clean cold critical load; that is, before the reactor is loaded to the hot critical configuration and operated at design temperature and power.

Fast transients (reactivity inputs $\geq$\$1) in UHTREX will require additional instrumentation and a faster rod withdrawal speed. Since this involves modifications to the present design, fast transients (if approved) would be done after all steady-state experiments at design power and temperature are completed. The fast transient work would, again, be done with the cold critical load, which is removed from the reactor in the process of loading to the design temperature critical load. Thus, the fission product inventory for the fast transient experiments would be only the small amount accumulated during the slow transient experiments which has not decayed during the intervening time.

GENERAL CALCULATIONAL METHOD

The transients described in this report were calculated with a reactor neutronics code based on analytic continuation (ANCON).[2] These transients are solutions to the conventional point kinetic equations with six delayed neutron groups:

$$\dot{N}(t) = \Lambda^{-1}[\rho(t) - \beta]\, N(t) + \sum_{i=1}^{6} \lambda_i\, \theta_i(t), \qquad (1)$$

$$\dot{\theta}_i(t) = \Lambda^{-1}\, \beta_i\, N(t) - \lambda_i\, \theta_i(t) \qquad (i=1,\ldots,6), \qquad (2)$$

and

$$\rho(t) = I(t) + F(t), \qquad (3)$$

where the impressed reactivity function I(t) is given by a polynomial in t of specified order L,

$$I(t) = \sum_{\ell=0}^{L} a_\ell\, t^\ell \qquad (0 \leq t \leq t_{max})$$

$$= \sum_{\ell=0}^{L} a_\ell\, t_{max}^\ell \qquad (t > t_{max}), \qquad (4)$$

and the feedback function F(t) is given by

$$F(t) = \sum_{j=1}^{J} \alpha_j [T_j(t) - T_j(0)], \qquad (5)$$

where J is the number of lumps in the feedback model and α_j is the reactivity coefficient of lump j.

The average temperature, $T_j(t)$, of lump j is described by a heat-balance equation of the type

$$C_j \dot{T}_j(t) = Q_j\, P(t) - \sum_i h_c^{j\to i}[T_j(t) - T_i(t)] - \sum_i h_r^{j\to i}[T_j^4(t) - T_i^4(t)] \qquad (i=1,\ldots,J), \qquad (6)$$

where

- C_j = heat capacity of lump j,
- Q_j = fraction of fission energy deposited in lump j,
- $P(t)$ = power level which is proportional to the neutron level, N(t),
- $h_c^{j\to i}$ = conductive or convective heat transfer coefficient from lump j to lump i, and
- $h_r^{j\to i}$ = radiative heat transfer coefficient from lump j to lump i.

Reactivity coefficients and heat capacities for the various lumps can be functions of temperature. The temperature dependence is expressed in terms of a polynomial in $T_j(t) - \bar{T}_j(0)$ of specified order:

$$\alpha_j(T_j) = \sum_{i=0}^{I_j} \gamma_{ji} [T_j(t) - T_j(0)]^i \qquad (7)$$

$$C_j(T_j) = \sum_{i=0}^{K_j} \delta_{ji} [T_j(t) - T_j(0)]^i. \qquad (8)$$

The neutronic constants used in the calculations are given in Table I. Constants appearing in the

TABLE I

NEUTRONIC CONSTANTS

$\Lambda = 9.643 \times 10^{-4}$ sec $\quad \beta = 6.7851 \times 10^{-3}$

β_i	λ_i (sec)$^{-1}$
2.2255×10^{-4}	1.2440×10^{-2}
1.4819×10^{-3}	3.0510×10^{-2}
1.3340×10^{-3}	1.1144×10^{-1}
2.6781×10^{-3}	3.0137×10^{-1}
7.8300×10^{-4}	1.1363
2.8565×10^{-4}	

feedback equations are given in the Appendix, where the various feedback models used in the calculations are described.

NUMERICAL RESULTS

Feedback Model Study

In an attempt to determine the importance of gross spatial variations in the reactivity coefficients and in the power (unrodded critical mode), results for step inputs of reactivity were obtained with three different feedback models, which are described in detail in the Appendix. The first is a 2-lump model in which the core is represented by one region containing one fuel lump and one moderator lump. Thus, spatial variations in reactivity coefficients and power are not taken into account in this model. The second is an 8-lump model in which the core is represented by four annular regions. This model approximates the radial variation in reactivity coefficients and power. The third is a 56-lump model in which the core is represented by 28 regions (four radial and seven axial zones). This model approximates both the radial and axial variations in the reactivity coefficients and power. The power distribution for the unrodded critical reactor was computed in two space dimensions (R-Z) and S_4 approximation with the DDK code.[3] Regular and adjoint S_n calculations for this configuration were used in the DAC code[4] to compute distributed reactivity coefficients by perturbation theory.

The graphite heat capacity and reactivity coefficients were assumed to be independent of temperature in the feedback model study. Also, the reactor was assumed to be under one atmosphere of helium. These conditions will be referred to as Case A.

Table II presents the results obtained with the three feedback models for step inputs in the range 10 to 90 cents. Results for the 10- and 90-cent cases are plotted in Figs. 1-3. Results obtained with the 8-lump model agree well with those obtained with the 56-lump model. Thus, the 8-lump model is adequate for detailed calculations. The 2-lump model, on the other hand, is adequate for survey calculations. The results are relatively insensitive to the feedback model used because fuel-element powers and the reactivity coefficients do not vary greatly with position in the core. Calculations described in subsequent sections of this report were all done with the 2-lump feedback model.

TABLE II

RESULTS FOR 2-, 8-, AND 56-LUMP FEEDBACK MODELS

Case A for Step Inputs of Reactivity

Reactivity	Peak Power (MW)			Time at Peak Power (sec)			Energy Release to Peak (MW-sec)		
(cents)	2 Lumps	8 Lumps	56 Lumps	2 Lumps	8 Lumps	56 Lumps	2 Lumps	8 Lumps	56 Lumps
10	0.0284	0.0252	0.0250	1178	1170	1170	6.45	5.83	5.79
30	0.236	0.219	0.217	265	262	262	11.0	10.7	10.6
50	0.787	0.765	0.754	96.7	96.0	96.0	14.1	13.1	13.2
70	2.02	2.09	1.97	41.1	40.6	40.8	16.3	14.8	15.6
90	5.52	5.48	5.43	19.0	18.9	18.9	17.7	17.3	17.2

Reactivity	Total Energy Release (MW-sec)			Average Fuel Temperature Rise at Peak Power (°C)			Maximum Average Fuel Temperature Rise (°C)		
(cents)	2 Lumps	8 Lumps	56 Lumps	2 Lumps	8 Lumps	56 Lumps	2 Lumps	8 Lumps	56 Lumps
10	16.1	14.7	14.6	15.2	17.6	17.4	16.5	19.6	19.4
30	42.1	37.5	37.3	73.1	73.6	73.0	96.0	104	103
50	64.7	58.1	57.6	121	117	118	207	216	214
70	86.0	78.0	77.4	158	146	154	332	343	344
90	107	97.8	97.1	180	178	176	465	476	472

Reactivity	Average Moderator Temperature Rise at Peak Power (°C)			Asymptotic Core Temperature Rise (°C)			Fraction of Feedback due to Fuel at Peak Power		
(cents)	2 Lumps	8 Lumps	56 Lumps	2 Lumps	8 Lumps	56 Lumps	2 Lumps	8 Lumps	56 Lumps
10	2.04	1.72	1.70	6.19	5.67	5.62	0.363	0.409	0.410
30	2.18	1.73	1.71	16.2	14.5	14.4	0.719	0.729	0.729
50	1.43	1.18	1.18	24.9	22.4	22.2	0.866	0.864	0.865
70	1.04	0.85	0.90	33.1	30.0	29.8	0.921	0.919	0.920
90	0.82	0.75	0.75	41.2	37.7	37.4	0.944	0.943	0.943

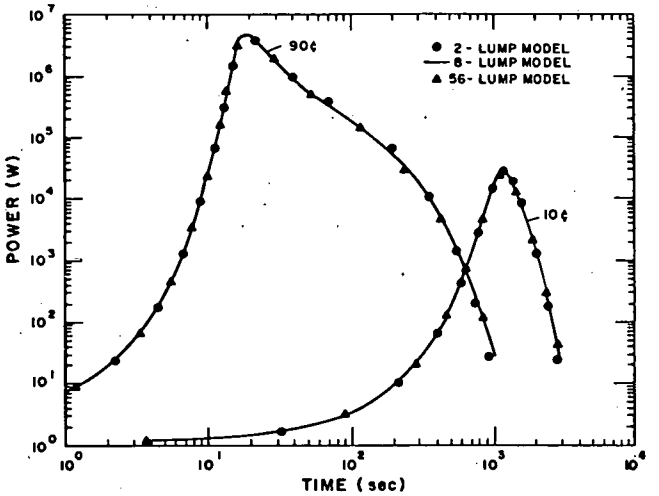

Fig. 1. Powers obtained with the three feedback models for Case A.

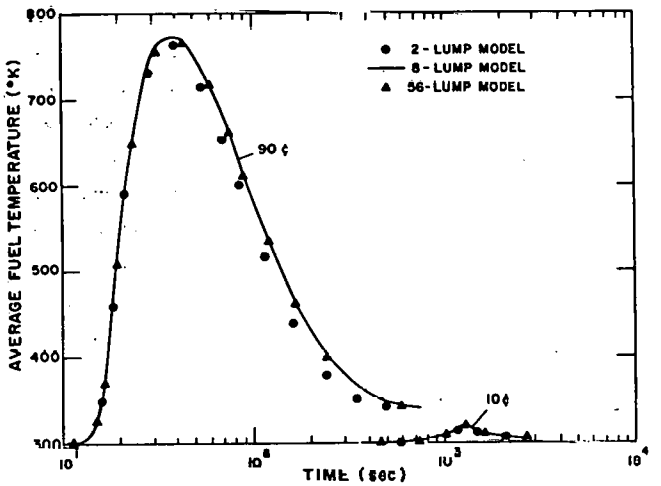

Fig. 2. Average fuel temperatures obtained with the three feedback models for Case A.

The values for the total energy release, maximum rise in the average fuel temperature, and asymptotic core temperature rise correspond to the case where there is no scram following the power peak. In order to minimize the waiting period between transients, during which time the core returns to room temperature, it is expected that the reactor will be scrammed after the power peak is reached.

TABLE III

PEAK-TO-AVERAGE TEMPERATURE RISE AT PEAK POWER

Reactivity (cents)	Fuel			Moderator		
	8 Lumps (radial)	56 Lumps (radial)	56 Lumps (axial)	8 Lumps (radial)	56 Lumps (radial)	56 Lumps (axial)
10	1.650	1.650	1.099	1.396	1.396	1.055
30	1.273	1.276	1.102	1.602	1.606	1.075
50	1.109	1.124	1.102	1.534	1.553	1.069
70	1.049	1.067	1.103	1.366	1.440	1.056
90	1.028	1.028	1.103	1.215	1.216	1.026

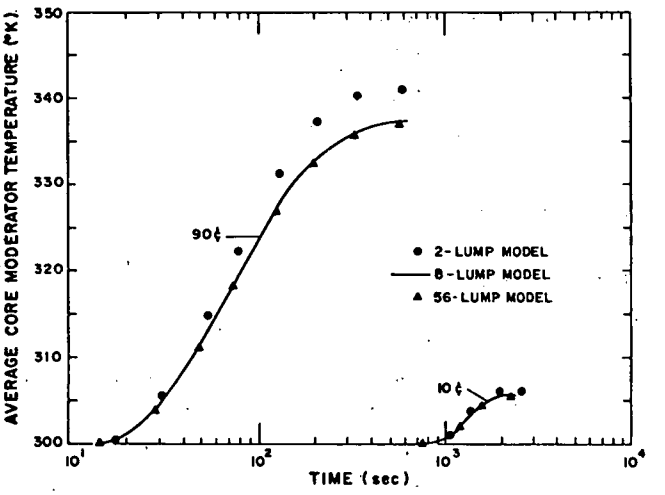

Fig. 3. Average core moderator temperatures obtained with the three feedback models for Case A.

Table III gives the core peak-to-average fuel and moderator temperature rises at peak power for the 8- and 56-lump models. These values do not take into account the temperature distribution within lumps; for example, within a fuel element.

Temperature-Dependent Heat Capacities and Reactivity Coefficients

The effect of variation with temperature of heat capacities and reactivity coefficients was studied with the 2-lump feedback model for step inputs of reactivity in the range 10 to 90 cents. Two cases were compared with Case A (in which the heat capacities and reactivity coefficients are assumed to be independent of temperature.)

The first case, referred to as Case B, is the same as Case A, except that the variation with

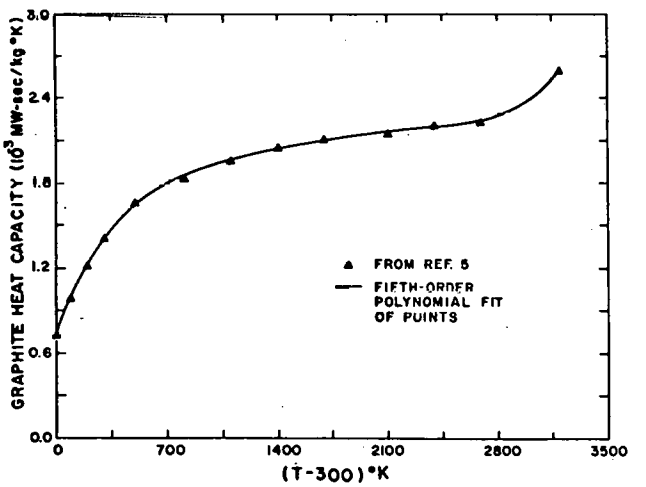

Fig. 4. Variation of graphite heat capacity with temperature.

TABLE IV

VALUES OF THE COEFFICIENTS a_n IN THE HEAT CAPACITY POLYNOMIAL

$$C(T) = \sum_{n=0}^{5} a_n (T - 300)^n$$

	Fuel Lump	Moderator Lump
a_0	8.63151×10^{-2}	2.50667
a_1	3.67802×10^{-4}	1.06985×10^{-2}
a_2	-3.94249×10^{-7}	-1.15115×10^{-5}
a_3	2.33248×10^{-10}	6.82406×10^{-9}
a_4	-6.96490×10^{-14}	-2.03902×10^{-12}
a_5	8.18053×10^{-18}	2.39435×10^{-16}

temperature of the heat capacities of the two lumps was taken into account. The heat capacity of graphite, which increases by a factor of 3.6 between 300° and 3500°K, as shown in Fig. 4, was used for both the fuel and moderator lumps. The points in Fig. 4 were taken from Reference 5 and agree with the values used in a system dynamics study[6] of UHTREX. The solid line in the figure is a fifth-order polynomial fit of the points. Such a polynomial (see Eq. 8) was used in the calculations to represent the variation of the heat capacity of each of the two lumps. The coefficients of the polynomials are given in Table IV, where the heat capacity is expressed in MW-sec/°K and T is in °K.

The second case, referred to as Case C, is the same as Case B, except that the reactivity coefficients were assumed to decrease linearly by a factor of 1.5 between 300° and 1800°K. (This is a reasonable estimate for UHTREX.) In other words, the reactivity coefficients for the fuel and moderator lumps were represented in the calculations by the first-order polynomials (Eq. 7)

$$\alpha_f = -1.402 \times 10^{-5} + 3.11555 \times 10^{-9}[T_f - 300]$$

and

$$\alpha_m = -1.8346 \times 10^{-4} + 4.07688 \times 10^{-8}[T_m - 300]$$

for $300 \leq T \leq 1800$°K.

Results for Cases A, B, and C are compared in Table V. These results show that, for the reactivity inputs considered, the heat capacity variation with temperature is relatively more important (with regard to all quantities compared except fuel temperature) than the assumed variation in the reactivity coefficients. Results for the 10- and 90-cent cases are also plotted in Figs. 5-7.

TABLE V

COMPARISON OF CASES A, B, AND C FOR STEP INPUTS OF REACTIVITY

2-Lump Feedback Model

Reactivity (cents)	Peak Power (MW)			Time at Peak Power (sec)			Energy Release to Peak (MW-sec)		
	Case A	Case B	Case C	Case A	Case B	Case C	Case A	Case B	Case C
10	0.0284	0.0286	0.0287	1178	1179	1186	6.45	6.50	6.71
30	0.236	0.265	0.268	265	270	270	11.8	13.7	13.8
50	0.787	0.979	1.00	96.7	100	101	14.1	18.6	19.8
70	2.02	2.71	2.82	41.1	43.4	43.8	16.3	24.7	26.1
90	5.52	7.35	7.72	19.0	20.2	20.3	17.7	28.6	29.6

Reactivity (cents)	Total Energy Release (MW-sec)			Average Fuel Temperature Rise at Peak Power (°C)			Maximum Average Fuel Temperature Rise (°C)		
	Case A	Case B	Case C	Case A	Case B	Case C	Case A	Case B	Case C
10	16.1	16.2	16.3	15.2	15.2	15.4	16.5	16.5	16.6
30	42.1	45.4	45.8	73.1	73.2	73.5	96.0	98.2	99.4
50	64.7	76.2	78.2	121	122	128	207	210	216
70	86.0	110	116	150	168	175	332	333	350
90	107	148	160	180	197	203	465	462	495

Reactivity (cents)	Average Moderator Temperature Rise at Peak Power (°C)			Asymptotic Core Temperature Rise (°C)			Fraction of Feedback due to Fuel at Peak Power		
	Case A	Case B	Case C	Case A	Case B	Case C	Case A	Case B	Case C
10	2.04	2.04	2.11	6.19	6.17	6.18	0.363	0.363	0.357
30	2.18	2.34	2.35	16.2	16.5	16.6	0.719	0.705	0.702
50	1.43	1.71	1.84	24.9	26.2	26.8	0.866	0.845	0.838
70	1.04	1.46	1.56	33.1	36.1	37.7	0.921	0.898	0.892
90	0.82	1.25	1.30	41.2	46.4	49.6	0.944	0.923	0.919

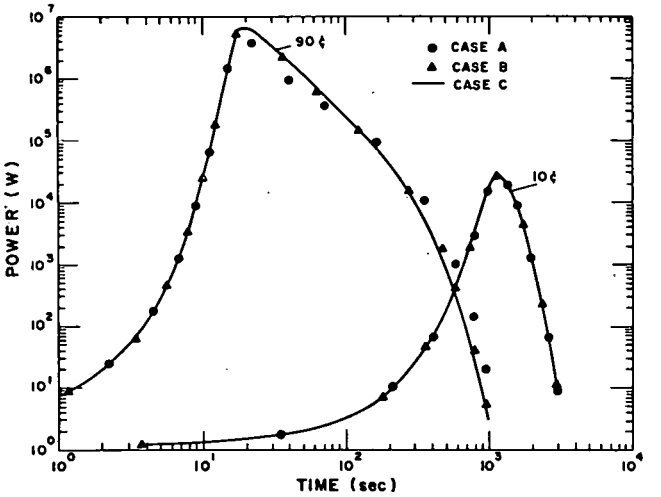

Fig. 5. Powers obtained with the 2-lump feedback model for Cases A, B, and C.

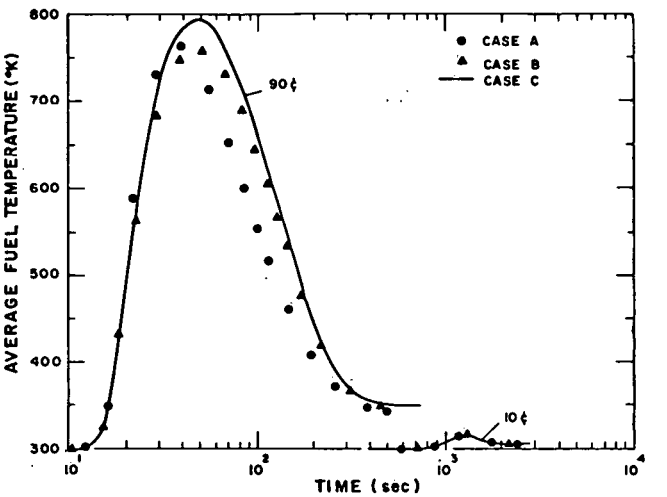

Fig. 6. Average fuel temperatures obtained with the 2-lump feedback model for Cases A, B, and C.

Comparison of Step Inputs with Slow Inputs of Reactivity

Results for step inputs of reactivity were compared with results for detailed reactivity inputs (due to withdrawal of a plug rod at 18 in./min). The 2-lump feedback model was used for this comparison.

The reactivity input as a function of time was calculated from experimental plug rod worth versus position data obtained in the UCX.[7] The total worth of the plug rod was assumed to be $4. In each transient, the initial position of the rod is such that, when it is withdrawn to an inactive position (50 in. from the fully inserted position), the desired reactivity is inserted. Initial positions of the plug rod, relative to the fully inserted position, are given in Table VI for various reactivity inputs. The final position in each case is 50 in. Figure 8 shows the impressed

TABLE VI

INITIAL PLUG ROD POSITIONS

Reactivity Input (cents)	Initial Plug Rod Position (in.)
0	50.0 (inactive position)
10	43.1
30	36.5
50	33.2
70	30.8
90	28.4
100	27.5
200	19.7
300	11.9
400	0.0 (fully inserted)

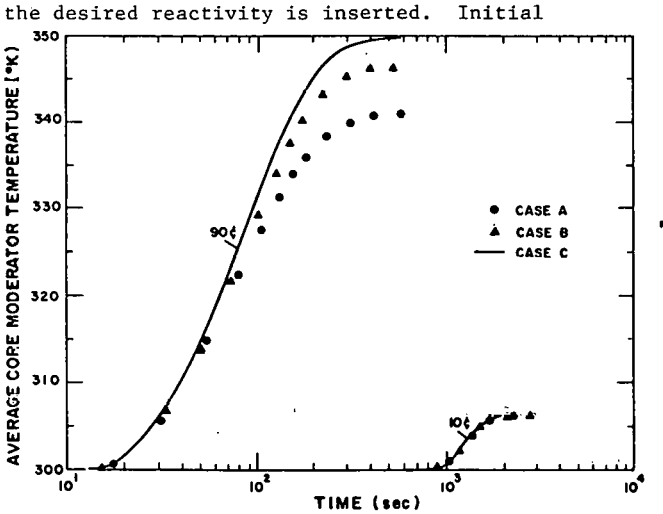

Fig. 7. Average core moderator temperatures obtained with the 2-lump feedback model for Cases A, B, and C.

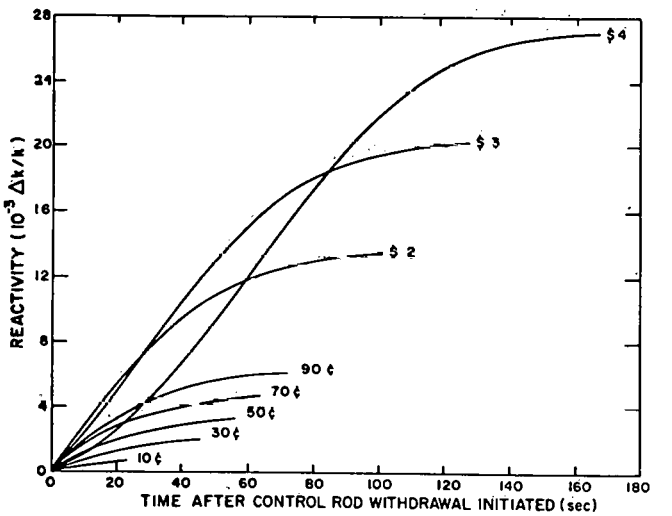

Fig. 8. Impressed reactivity due to plug rod withdrawal at 18 in./min from various initial positions.

reactivity functions for the various initial plug rod positions.

In the calculations, the curves in Fig. 8 were represented by polynomials in t (see Eq. 4). Coefficients of the polynomials and t_{max}, which is the time required to withdraw the rod to the inactive position, are given in Table VII.

Results of the calculations are given in Table VIII. Case C was used for input reactivities up to 90 cents, and Case B was used for the larger

TABLE VII

COEFFICIENTS OF IMPRESSED REACTIVITY POLYNOMIAL (Eq. 4)

Reactivity (cents)	a_0	a_1	a_2	a_3	a_4	a_5	a_6	a_7	t_{max} (sec)
10	0	2.9500-05	---	---	---	---	---	---	23
30	0	7.7416-05	-7.1516-07	---	---	---	---	---	45
50	0	1.5141-04	-2.7759-06	2.0607-08	---	---	---	---	56
70	0	1.9585	-3.1649	1.9756-08	---	---	---	---	64
90	0	2.0093	-2.0542	6.1331-09	---	---	---	---	72
100	0	2.0864	-1.1832	-2.3959-08	2.4969-10	---	---	---	75
200	0	2.9371	-7.0291-07	-2.3743-08	1.5747-10	-8.0672-14	---	---	101
300	0	3.1978	-4.8465-06	1.6850-07	-2.7025-09	1.8194-11	-4.4163-14	---	127
400	0	1.3171	-2.2300-06	1.4706-07	-2.3522-09	1.7626-11	-6.7932-14	1.0935-16	167

TABLE VIII

COMPARISON OF STEP INPUTS OF REACTIVITY AND ROD WITHDRAWAL AT 18 in./min

2-Lump Model

Reactivity (cents)	Peak Power (MW)		Time at Peak Power (sec)		Energy Release to Peak (MW-sec)	
	Step	18 in./min	Step	18 in./min	Step	18 in./min
10	0.0287	0.0287	1186	1198	6.71	6.71
30	0.268	0.268	270	291	13.8	13.9
50	1.00	1.00	101	128	19.8	19.8
70	2.82	2.79	43.8	77.2	26.1	27.3
90	7.72	5.49	20.3	56.7	29.6	34.8
100	12.5	5.79	14.4	51.0	29.7	30.7
200	289	21.8	2.82	31.4	89.7	34.8
300	1139	24.2	1.57	30.9	182	34.1

Reactivity (cents)	Total Energy Release (MW-sec)		Average Fuel Temp. Rise at Peak Power (°C)		Maximum Average Fuel Temp. Rise (°C)	
	Step	18 in./min	Step	18 in./min	Step	18 in./min
10	16.3	16.3	15.4	15.4	16.6	16.6
30	45.8	45.8	73.5	74.1	99.4	99.4
50	78.2	78.2	128	128	216	216
70	116	116	175	182	350	350
90	160	156	203	226	495	479
100	168	157	206	204	526	473
200	397	280	495	235	1171	729
300	584	365	929	251	1804	818

Reactivity (cents)	Average Moderator Temp. Rise at Peak Power (°C)		Asymptotic Core Temp. Rise (°C)		Fraction of Feedback due to Fuel at Peak Power	
	Step	18 in./min	Step	18 in./min	Step	18 in./min
10	2.11	2.11	6.18	6.18	0.357	0.358
30	2.35	2.38	16.6	16.6	0.702	0.700
50	1.84	1.85	26.8	26.8	0.838	0.837
70	1.56	1.65	37.7	37.7	0.892	0.890
90	1.30	1.68	49.6	48.7	0.919	0.907
100	1.18	1.39	51.7	49.0	0.930	0.918
200	2.77	1.24	106	81.8	0.932	0.935
300	5.50	1.23	170	115	0.928	0.940

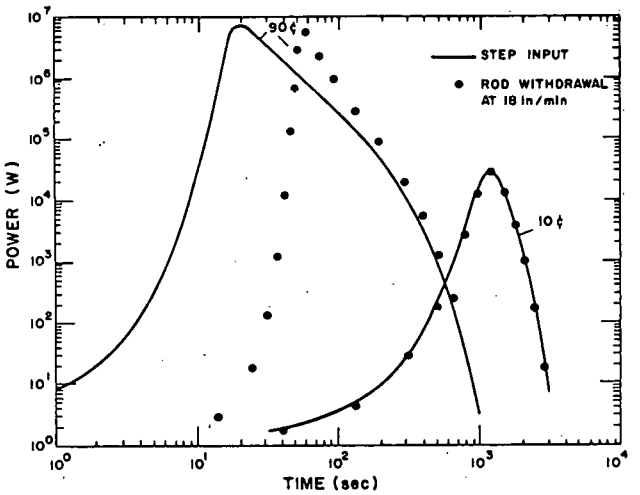

Fig. 9. Powers for step inputs and slow inputs of reactivity. Case C with 2-lump feedback model.

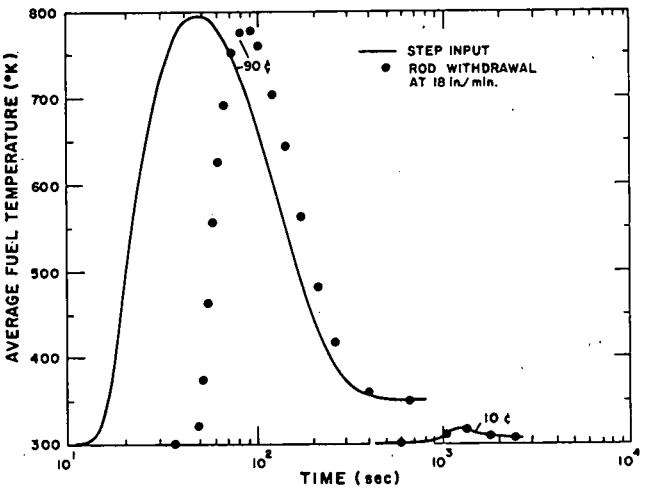

Fig.11. Average core moderator temperatures for step inputs and slow inputs of reactivity. Case C with 2-lump feedback model.

reactivity inputs. Results for the 10- and 90-cent inputs are plotted in Figs. 9-11. In addition, the initial asymptotic reactor period for various step inputs of reactivity is given in Table IX. This quantity is, by definition, the stable reactor period established before temperature feedback occurs. It is thus independent of the feedback model.

Table VIII shows that, for reactivity inputs up to 70 cents, the peak power is less than the UHTREX nominal design power of 3 MW. For step inputs from 10 to 70 cents, Table IX shows that the stable period ranges from 100 to 2.56 sec. In addition, Table VIII indicates that insertion of up to 70 cents by control rod withdrawal at 18 in./min

TABLE IX

INITIAL ASYMPTOTIC PERIOD FOR VARIOUS STEP INPUTS OF REACTIVITY

Reactivity (cents)	Period (sec)
10	100
30	18.9
50	6.41
70	2.56
90	1.12
100	0.787
200	0.136
300	0.0699

yields the same results as step inputs, except for the time to peak power.

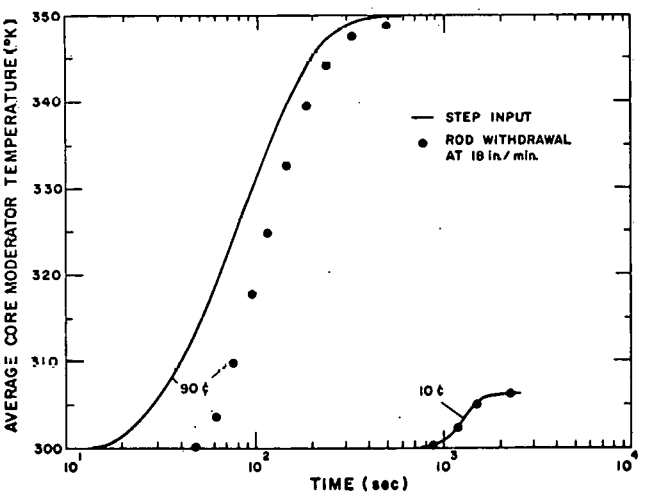

Fig. 10. Average fuel temperatures for step inputs of reactivity. Case C with 2-lump feedback model.

For reactivity inputs of 90 cents or more by rod withdrawal at 18 in./min, the excursion reaches peak power before all the reactivity has been inserted. In other words, thermal feedback terminates the excursion before the rod has reached the inactive position. This can be seen by comparing the time to peak power in Table VIII with the time required to withdraw the rod (t_{max} in Table VII). The reactivity inserted by the rod before thermal feedback terminates the excursion is given in Table X for the various initial plug rod positions. Also given is the maximum positive net reactivity achieved during the transient. These data show that the maximum possible reactivity insertion to peak power by rod withdrawal at 18 in./min is about 120 cents. Furthermore, the maximum positive net reactivity which can be achieved is about 110 cents. Thus, shorter rod withdrawal times will be required

TABLE X

REACTIVITY INSERTION TO PEAK POWER BY ROD WITHDRAWAL AT 18 in./min

Initial Plug Rod Position (in.)	Reactivity Held Down by Rod (cents)	Reactivity Insertion to Peak Power (cents)	Maximum Positive Net Reactivity During Transient (cents)
43.1	10	10	10
36.5	30	30	30
33.2	50	50	50
30.8	70	70	68
28.4	90	87.0	80.5
27.5	100	89.5	83.4
19.7	200	117.1	106.2
11.9	300	121.4	108.8
0.0	400	119.8	104.9

to initiate fast transients. In order to simulate steps up to \$3, the rod withdrawal time should be 1 sec or less. This can be achieved with an acceleration of 1 g.

For a \$3 step input, Table VIII shows that the maximum average fuel temperature is 2100°K. Calculations with a heat transfer model for the triplex-coated particles[8] imbedded in the fuel elements indicate that the peak temperature within the particle kernels will reach the melting point (2530°K) of UC_2. Thus, the maximum step input of reactivity that can be inserted without melting the fuel particle kernels is less than \$3.

Transients with Helium Replaced by Nitrogen or a Vacuum

Results obtained with helium replaced by nitrogen or a vacuum and results obtained with the reactor under one atmosphere of helium are given in Table XI for Case B. The calculations were done with the 2-lump feedback model for step inputs of reactivity from 10 to 90 cents.

Since the thermal conductivity of nitrogen is one-fifth that of helium, replacement of helium with nitrogen will reduce the heat transfer by conduction from the fuel elements to the core moderator. With helium replaced by a vacuum, the heat transfer is entirely by radiation. Thus, nitrogen or a vacuum will aid in isolating the fuel temperature coefficient from the moderator coefficient,

TABLE XI

COMPARISON OF RESULTS FOR STEP INPUTS OF REACTIVITY WITH HELIUM, NITROGEN, AND A VACUUM

Case B with 2-Lump Feedback Model

Reactivity (cents)	Peak Power (MW)			Time at Peak Power (sec)			Energy Release to Peak (MW-sec)		
	He	N	Vacuum	He	N	Vacuum	He	N	Vacuum
10	0.0286	0.0227	0.0194	1186	1163	1143	6.69	5.30	4.47
30	0.265	0.241	0.234	270	268	268	13.7	12.4	12.1
50	0.979	0.946	0.937	100	99.9	99.9	18.6	18.1	18.0
70	2.71	2.70	2.70	43.4	43.2	43.2	24.7	23.7	23.7
90	7.35	7.21	7.13	20.2	19.9	19.8	28.6	26.7	25.7

Reactivity (cents)	Total Energy Release (MW-sec)			Average Fuel Temp. Rise at Peak Power (°C)			Maximum Average Fuel Temp. Rise (°C)		
	He	N	Vacuum	He	N	Vacuum	He	N	Vacuum
10	16.2	13.6	10.9	15.4	29.7	38.5	16.5	37.6	64.0
30	45.4	39.8	37.8	73.2	90.8	97.0	98.2	162	204
50	76.2	71.3	70.3	122	134	137	210	291	334
70	110	107	107	168	171	173	333	419	457
90	148	146	146	197	191	186	462	545	578

Reactivity (cents)	Average Moderator Temp. Rise at Peak Power (°C)			Asymptotic Core Temp. Rise (°C)			Fraction of Feedback due to Fuel at Peak Power		
	He	N	Vacuum	He	N	Vacuum	He	N	Vacuum
10	2.10	1.01	0.325	6.17	5.15	4.12	0.363	0.692	0.901
30	2.34	0.943	0.489	16.5	14.3	13.8	0.705	0.880	0.938
50	1.71	0.856	0.612	26.2	25.0	24.8	0.845	0.923	0.945
70	1.46	0.892	0.753	36.1	36.0	36.0	0.898	0.936	0.946
90	1.25	0.893	0.792	46.4	46.4	46.4	0.923	0.942	0.947

especially for the smaller reactivity inputs. This can be seen by comparing the feedback fractions due to the fuel at peak power in Table XI. No significant increases in fuel feedback fraction are to be expected for inputs greater than 90 cents, because the power peak is reached before much heat can be transferred in any case.

Sensitivity of Results to Arbitrary Changes in Λ and Reactivity Coefficients

In order to study the sensitivity of calculated results to changes in the prompt neutron generation time (Λ) and fuel and moderator reactivity coefficients (α_f and α_m), arbitrary changes in these quantities were made, and calculations were performed for step inputs of reactivity in the range 10 to 90 cents. The calculations were done with the 2-lump feedback model for Case B.

The results of these calculations are presented in Table XII. Four sets of calculations are included in the table. They are for

a. The reference case,
b. The reference case with 0.8 Λ,
c. The reference case with 0.8 α_f, and
d. The reference case with 0.8 α_m.

An examination of Table XII shows that, for the reactivity inputs considered, the change in Λ has little effect on any of the quantities compared. The change in α_m can be seen to affect mostly the fraction of the feedback due to the fuel and the energy release. In general, the results are most sensitive to the change in α_f. This is desirable since one of the purposes of the transients is to verify the calculated value for α_f.

APPENDIX. THE FEEDBACK MODELS

The three different core thermal feedback models used in the calculations are described in this appendix. Because the transients are conducted with an unpressurized system with no coolant flow, heat transfer from the core to the surrounding reflector regions during the transients can be neglected. Thus, the feedback models represent only the core of the reactor.

Values for heat capacities, reactivity coefficients, and conductive heat transfer coefficients given in this appendix are all computed at 300°K. Also, the conductive heat transfer coefficients between lumps are based on the following values for

TABLE XII

STEP INPUTS OF REACTIVITY

Case B with 2-Lump Feedback Model

Reactivity (cents)	Peak Power (MW)				Time to Peak Power (sec)				Energy Release to Peak (MW-sec)			
	(a)	(b)	(c)	(d)	(a)	(b)	(c)	(d)	(a)	(b)	(c)	(d)
10	0.0286	0.0287	0.0312	0.0326	1179	1182	1189	1204	6.50	6.69	7.17	7.77
30	0.265	0.264	0.315	0.281	270	267	272	272	13.7	13.5	16.0	14.8
50	0.979	0.985	1.21	1.01	100	98.1	101	100	18.6	18.6	23.0	19.5
70	2.71	2.80	3.47	2.80	43.4	41.0	43.8	43.3	24.7	22.8	30.3	24.7
90	7.35	7.87	9.18	7.30	20.2	18.2	20.0	19.8	28.6	25.6	32.2	26.2

Reactivity (cents)	Total Energy Release (MW-sec)				Average Fuel Temperature Rise at Peak Power (°C)				Maximum Average Fuel Temperature Rise (°C)			
	(a)	(b)	(c)	(d)	(a)	(b)	(c)	(d)	(a)	(b)	(c)	(d)
10	16.2	16.2	17.1	19.3	15.2	15.4	16.7	17.6	16.5	16.6	17.9	18.9
30	45.4	45.2	50.2	52.1	73.2	72.8	84.1	77.8	98.2	98.2	114	105
50	76.2	76.0	87.6	85.5	122	122	146	127	210	210	248	220
70	110	110	131	122	168	158	199	168	333	334	397	345
90	148	148	179	162	197	181	217	184	462	462	552	474

Reactivity (cents)	Average Moderator Temperature Rise at Peak Power (°C)				Asymptotic Core Temperature Rise (°C)				Fraction of Feedback due to Fuel at Peak Power			
	(a)	(b)	(c)	(d)	(a)	(b)	(c)	(d)	(a)	(b)	(c)	(d)
10	2.04	2.11	2.25	2.45	6.17	6.17	6.48	7.30	0.363	0.359	0.312	0.408
30	2.34	2.31	2.67	2.53	16.5	16.5	18.0	18.8	0.705	0.707	0.658	0.746
50	1.71	1.70	2.08	1.80	26.2	26.2	29.6	29.3	0.845	0.846	0.811	0.870
70	1.46	1.32	1.76	1.45	36.1	36.2	41.7	39.7	0.898	0.902	0.873	0.917
90	1.25	1.10	1.37	1.12	46.4	46.6	54.5	50.4	0.923	0.926	0.907	0.941

a. Reference case.
b. Reference case with 0.8 Λ.
c. Reference case with 0.8 α_f.
d. Reference case with 0.8 α_m.

the conductivities of various materials at 300°K:

Material	k(MW/cm°K)
Core moderator[9]	1.6265×10^{-6}
Fuel elements[9]	5.19×10^{-7}
Helium (1 atm)[10]	1.53×10^{-9}

2-Lump Model

In the 2-lump model, the entire core is represented by a fuel lump and a moderator lump. The core moderator (a hollow cylinder 99.06 cm high, inner radius 29.21 cm, and outer radius 88.9 cm) has a total graphite mass of 3468 kg. In obtaining this mass, the moderator graphite density was taken as 1.73 g/cm^3, and the fuel channel and core rod holes were taken into account. The fuel elements (1248 hollow cylinders 13.97 cm long, inner radius 0.635 cm, and outer radius 1.27 cm) contain a total of 119.6 kg of graphite of 1.805 g/cm^3 density. The four fuel elements within a channel extend from an inner radius of 29.997 cm to an outer radius of 85.877 cm, measured from the center of the hollow core moderator cylinder.

Parameters used in the feedback equations for this model are given in Table A.I. Lump 1 represents the fuel elements, and lump 2 represents the core moderator.

8-Lump Model

In this model, the core is divided into four annular regions whose outer radii are:

Region 1 R = 43.967 cm
2 R = 57.937 cm
3 R = 71.907 cm
4 R = 88.9 cm.

Each annular region extends over the full height of the core.

TABLE A.I

PARAMETERS FOR 2-LUMP FEEDBACK MODELS

Lump i	Q_i	C_i(MW-sec/°K)	$-\alpha_i$(Δk/k/°K)	$h_r^{1\to2}$(MW/°K^4)	$h_c^{1\to2}$(MW/°K)
1	0.925	0.0867	1.402×10^{-5}	6.368×10^{-13}	1.7263×10^{-3}
2	0.075	2.51	1.8346×10^{-4}		

Parameters used in the feedback equations for this model are given in Table A.II. Lumps 1 through 4 are, respectively, the fuel elements in regions 1 through 4, while lumps 5 through 8 are, respectively, the core moderator associated with regions 1 through 4.

The fission energy fraction (0.925) deposited in the fuel elements was distributed among lumps 1 through 4 according to fuel element power fractions computed by the DDK[3] code for regions 1 through 4. The fraction (0.075) of the fission energy deposited in the core moderator was distributed among lumps 5 through 8 according to the core moderator weight fractions in the four regions. Reactivity coefficients for each lump were obtained from spatial reactivity coefficient distributions computed by the DAC code.[4]

56-Lump Model

In the 56-lump model, the core is represented by 28 regions (four radial and seven axial zones) as shown in Fig. A.1. Azimuthal symmetry and symmetry about Channel 7 are assumed.

Table A.III lists the parameters used in the feedback equations for this model. Lumps 1 through 28 represent, respectively, the fuel elements in regions 1 through 28, while lumps 29 through 56 represent, respectively, the core moderator in regions 1 through 28.

TABLE A.II

PARAMETERS FOR 8-LUMP FEEDBACK MODEL

Lump j	Q_j	C_j(MW-sec/°K)	$-\alpha_j$(Δk/k/°K)	i	$h_r^{j\to i}$(MW/°K^4)	i	$h_c^{j\to i}$(MW/°K)
1	0.22191	0.02168	3.5545×10^{-6}	5	1.5920×10^{-13}	5	4.3236×10^{-4}
2	0.23319		3.5229	6		6	4.3182
3	0.23588		3.5036	7		7	4.3141
4	0.23402		3.4388	8		8	1.3093
5	0.01152	0.38554	5.4649×10^{-5}			6	3.1595×10^{-3}
6	0.01512	0.50602	4.8888			7	4.1777
7	0.01776	0.59437	4.3097			8	5.1939
8	0.03060	1.0241	3.6826				

TABLE A.III

PARAMETERS FOR 56-LUMP MODEL

Lump j	Q_j	C_j (MW-sec/°K)	$-\alpha_j$ ($\Delta k/k/°K$)	i	$h_r^{j\to i}$ (MW/°K^4)	i	$h_c^{j\to i}$ (MW/°K)
1	1.8875-02	1.6673-03	3.2285-07	29	1.2246-14	29	3.3258-05
2	3.7420	3.3347-03	6.3508	30	2.4492-14	30	6.6517-05
3	3.6470		6.0541	31		31	
4	3.4970		5.6090	32		32	
5	3.3115		5.1135	33		33	
6	3.1174		4.6715	34		34	
7	2.9829		4.5210	35		35	
8	1.9801	1.6673-03	3.1537	36	1.2246-14	36	3.3217-05
9	3.9252	3.3347-03	6.2022	37	2.4492-14	37	6.6434-05
10	3.8236		5.9093	38		38	
11	3.6648		5.4835	39		39	
12	3.4720		5.0353	40		40	
13	3.2822		4.7057	41		41	
14	3.1690		4.7435	42		42	
15	1.9991	1.6673-03	3.1329	43	1.2246-14	43	3.3185-05
16	3.9635	3.3347-03	6.1645	44	2.4492-14	44	6.6371-05
17	3.8631		5.8798	45		45	
18	3.7060		5.4649	46		46	
19	3.5177		5.0274	47		47	
20	3.3304		4.6811	48		48	
21	3.2116		4.6754	49		49	
22	1.9832	1.6673-03	3.1231	50	1.2246-14	50	1.0072-05
23	3.9332	3.3347-03	6.1458	51	2.4492-14	51	2.0143-05
24	3.8370		5.8647	52		52	
25	3.6859		5.4449	53		53	
26	3.4996		4.9673	54		54	
27	3.3057		4.5322	55		55	
28	3.1601		4.3142	56		56	
29	8.8612-04	2.9656-02	5.0242-06			30	1.3858-03
						36	2.4304-04
30	1.7723-03	5.9314-02	9.8786			31	1.3858-03
						37	4.8608-04
31			9.4005			32	1.3858-03
						38	4.8608-04
32			8.6778			33	1.3858-03
						39	4.8608-04
33			7.8519			34	1.3858-03
						40	4.8608-04
34			7.0843			35	1.3858-03
						41	4.8608-04
35			6.7313			42	4.8608-04
36	1.1631-03	3.8925-02	4.4539			37	1.9093-03
						43	3.2136-04
37	2.3261-03	7.7848-02	8.7543			38	1.9093-03
						44	6.4272-04
38	2.3261-03	7.7848-03	8.3225			39	1.9093-03
						45	6.4272-04
39			7.6835			40	1.9093-03
						46	6.4272-04
40			6.9797			41	1.9093-03
						47	6.4272-04
41			6.4017			42	1.9093-03
						48	6.4272-04
42			6.2936			49	6.4272-04
43	1.3661-03	4.5720-02	3.9048			44	2.4327-03
						50	3.9953-04
44	2.7323-03	9.1442-02	7.6785			45	2.4327-03
						51	7.9906-04
45			7.3101			46	2.4327-03
						52	7.9906-04
46			6.7655			47	2.4327-03
						53	7.9906-04
47			6.1718			48	2.4327-03
						54	7.9906-04
48			5.6867			49	2.4327-03
						55	7.9906-04
49			5.5794			56	7.9906-04
50	2.3539-03	7.8776-02	3.3498			51	2.9562-03
51	4.7077-03	1.5755-01	6.5908			52	
52			6.2857			53	
53			5.8300			54	
54			5.3101			55	
55			4.8389			56	
56			4.6201				

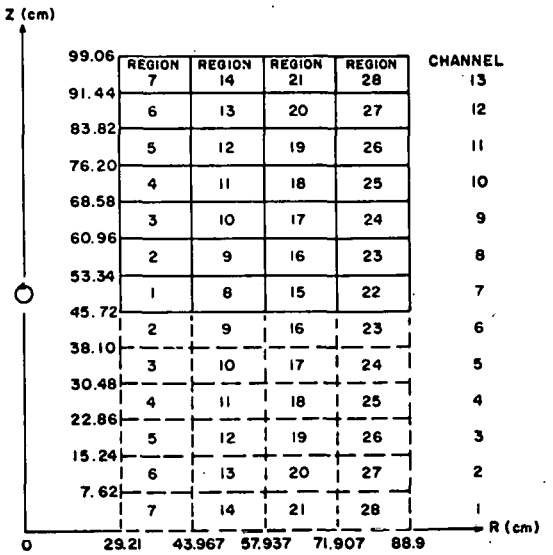

Fig. A.1. 28-region model for UHTREX core.

The Q_j and α_j in Table A.III were obtained in the manner described for the 8-lump model. Note that while the 8-lump model approximates the radial power distribution (unrodded critical mode) and radial reactivity coefficient distributions, the 56-lump model approximates both the radial and axial distributions.

REFERENCES

1. "Ultra High Temperature Reactor Experiment (UHTREX) Facility Description and Safety Analysis Report," Los Alamos Scientific Laboratory Report LA-3556 (Revised), 1967.

2. J. C. Vigil, "Solution of the Nonlinear Reactor Kinetics Equations by Continuous Analytic Continuation," Los Alamos Scientific Laboratory Report LA-3518, 1966.

3. W. J. Worlton and B. G. Carlson, "The DDK Code," an unpublished Los Alamos Scientific Laboratory code.

4. B. M. Carmichael, "The DAC Code," an unpublished Los Alamos Scientific Laboratory code.

5. R. E. Nightingale, Nuclear Graphite, Academic Press, New York, 1962.

6. H. B. Demuth et al., "System Dynamics Report for the Ultra High Temperature Reactor Experiment," Los Alamos Scientific Laboratory Report LA-3561, 1966.

7. B. M. Carmichael et al., "UCX Operations, June 21 through July 20, 1965," an unpublished Los Alamos Scientific Laboratory internal memorandum.

8. J. M. Taub and R. J. Bard, "Coated Particle Fuel Elements for UHTREX," Los Alamos Scientific Laboratory Report LA-3378, 1966.

9. P. Salgado, Personal Communication.

10. "The Physical and Thermodynamic Properties of Helium," Whittaker Controls Report, September 1960 (Revised).